O.V. Sobol'[1], H.O. Postelnyk[1], N.V. Pinchuk[1], A.A. Meylekhov[1], M.A. Zhadko[1],
A.A. Andreev[2], V.A. Stolbovoy[2]

Influence of Bias Potential Magnitude on Structural Engineering of ZrN-Based Vacuum-Arc Coatings

[1]*National Technical University "Kharkiv Polytechnic Institute", Kharkiv, Ukraine, sool@kpi.kharkov.ua*
[2]*National Science Center "Kharkiv Institute of Physics and Technology", Kharkiv, Ukraine, stolbovoy@kipt.kharkov.ua*

The creation of the scientific foundations for the structural engineering of ultrathin nanolayers in multilayer nanocomposites is the basis of modern technologies for the formation of materials with unique functional properties. It is shown that an increase in the negative bias potential (from -70 to -220 V) during the formation of vacuum-arc nanocomposites based on ZrN makes it possible not only to control the preferred orientation of crystallites and substructural characteristics, but also changes the conditions for conjugation of crystal lattices in ultrafine (about 8 nm) nanolayers.

Key words: vacuum arc, zirconium nitride, multilayer nanocomposites, X-ray structural analysis, nanostructure, interlayer conjugation, texture, substructure.

Introduction

In order to achieve high functional properties of materials, a new scientific direction "structural engineering of the surface" has become widespread in recent years in materials science [1-3]. This scientific direction is based on the establishment of a connection between the technological conditions for obtaining materials, their phase-structural state and basic functional properties. Thanks to the application of "structural engineering of the surface", it became possible to modify the phase-structural states of vacuum-arc coatings deposited in highly nonequilibrium conditions [4-6].

At the same time, two paths of structural design (structural engineering) were formed. The first one is based on the achievement of the necessary structural states and properties by creating multi-element coatings (as a result of directional alloying with elements necessary to achieve the properties) [7-9].

The second way is based on the creation of multilayer composites in which different materials of the layers, their thickness, the nature of interlayer interaction and other characteristics are used to achieve the required properties [10-11]. In this case, one of the important features of such multilayer coatings is the ability to combine the advantages of materials they are made of [12].

As has been shown in a number of studies, gradient and multilayer coatings obtained in this way, consisting of various nitride layers, demonstrate unique mechanical properties, such as high and ultra-high hardness and adhesion strength. This is largely determined by the formation of special boundaries between the layers, which fundamentally distinguishes such materials from single-layer coatings [13-17].

Among multilayer coatings, nanostructured coatings with a nanocrystalline structural state or nano-scale multi-period composites show the highest properties, since it is possible to create special boundaries for consistent (or inconsistent) deformation, as a result of which the physical and mechanical properties of the coatings significantly change [18-19].

Therefore, the aim of work was to study the effect of the negative bias potential applied to the substrate during deposition on the structure and substructure of a single-layer ZrN coating, as well as when using ZrN as

nanocomposite layers.

I. Materials and research methods

The coatings were deposited in a "Bulat-6" vacuum arc installation for 1.5 hours. As a base material, polished substrates made of 12Kh18N9T stainless steel with dimensions of 20x20x3 mm, which were preliminarily washed with an alkaline solution in an ultrasonic bath and then in C2-80/120 nefras, were used. After evacuating the vacuum chamber to a pressure of $1·10^{-5}$ Torr, a negative potential of 1000 V was applied to the substrates, and at an arc current of 100 A, their surface was cleaned and activated by bombardment with titanium ions for 3 ... 4 min. Then the chamber was filled with a nitrogen atmosphere until a working pressure $P_N = 4·10^{-3}$ Torr. During deposition, one of the main technological parameters was changable – negative bias potential (U_b), which was -70 V, -120 V and -220 V.

Zirconium (99.95 %) was used as the cathode in the formation of a single-layer coating. The same cathode was used for the formation of ZrN layers in multilayer coatings, and in coatings of this type of molybdenum nitride layers, molybdenum of the MChVP grade was used. For the zirconium cathode and (TiZr)N, the arc discharge current was 100 A, and for molybdenum, 130 A.

Multilayer coatings were obtained both by continuous rotation of the substrate holder at a speed of 8 rpm (with an average residence time in the cathode region of 3 - 4 sec.) and a number of layers of 540 - 570, and by a fixed stop for 40 sec. opposite each of the 2 cathodes to obtain thicker layers. The deposition rate of the coating was about 2 nm/s.

The deposition of multilayer coatings was carried out from two sources of evaporation, one of which is Zr or Mo, the second is TiZr (30 wt.% Zr). The thickness of the layers was determined by calculation based on the total thickness of the coating and the number of layers.

The total thickness of the coatings was about 10 μm.

The phase-structural state was studid using X-ray diffractometry techniques. X-ray diffraction spectra were obtained on the DRON-4 installation in Cu-K$_α$ radiation using θ - 2θ scanning in the range of angles 30...90°, with a scanning step of 0.1 deg and a holding time of 10 s. To monochromatize the detected radiation, a graphite monochromator installed in the secondary beam (in front of the detector) was used [20]. The division of complex profiles into components was carried out using the "NewProfile" software package. To determine the crystallographic structure and phase composition of the coatings, X-ray scans were performed and compared with the powder diffraction (JCPDS) files published by the International Center for Diffraction Data (ICDD) [21]. Substructural characteristics were determined by the approximation method [22].

II. Results and discussion

2.1. Influence of the bias potential on the structure and substructure of single-layer ZrN coatings

The value of the negative bias potential was used as a physical and technological parameter that changed during deposition. Since the degree of ionization of metal vapors in a vacuum arc discharge can reach almost 100 %, changing the bias potential is an effective way to influence the energy of the deposited particles. With a single ionization, the value of energy of the charged particles is close to the value of the bias potential.

First it will be considered how such a change in physical and technological parameters affects the structural state of single-layer ZrN coatings, about 8 μm thick.

Fig. 1 shows the diffraction spectra from coatings deposited at $U_b = -70$ V (spectrum 1), $U_b = -120$ V (spectrum 2) and $U_b = -220$ V (spectrum 3).

It can be seen from the obtained spectra that with

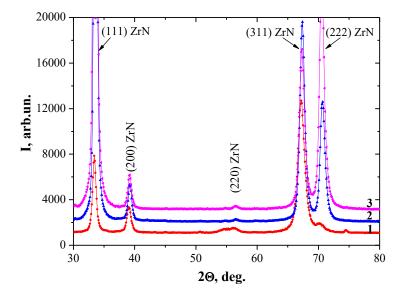**Fig. 1.** Diffraction spectra of single-layer ZrN coatings: 1 – $U_b = -70$ V, 2 – $U_b = -120$ V, 3 – $U_b = -220$ V.

O.V. Sobol', H.O. Postelnyk, N.V. Pinchuk, A.A. Meylekhov, M.A. Zhadko, A.A. Andreev, V.A. Stolbovoy

Table 1

Substructural characteristics (average crystallite size (L) and microstrain ($<\varepsilon>$)) in ZrN coatings obtained at different U_b

Series No	U_b, V	L, nm	$<\varepsilon>$, %
1	-70	50	0.69
2	-120	270	0.58
3	-220	300	0.65

increasing U_b, the relative intensity of the (111) and (222) peaks increases. This indicates the formation of a texture with the [111] axis and an increase in the degree of its perfection with increasing U_b. The substructural characteristics determined from the data on the change in half-width at different angles are summarized for different U_b in Table 1.

It can be seen from the results shown in Table 1 that an increase in U_b leads to the crystallite size growth. This is due to an increase in the energy of the deposited particles, which leads to an increase in the mobility of atoms. In this case, not only does the average crystallite size grows, but also the formation of a preferred growth orientation (texture, Fig. 1) parallel to the surface of crystallites with the (111) plane, in which the reticular density of atoms is highest, occurs. The value of microstrain $<\varepsilon>$ tends to decrease with increasing U_b (Table 1).

Thus, the influence of the bias potential (and, accordingly, the average energy of deposited particles) has a decisive effect on the formation of the preferred orientation of crystallites, substructural characteristics, and macrodeformation.

2.2. Multilayer periodic coatings based on zirconium nitride with nanometer-thick layers

As it was found, according to the data of X-ray fluorescence elemental analysis, in the (TiZr) layers the atomic ratio of the element content is 83/17 at $U_b = -70$ V

and 82/18 at $U_b = -120$ V. Based on this ratio, according to Vegard's law, the lattice period of the $(Ti_{0,83}Zr_{0,17})N$ nitride is approximately equal to 0.4306 nm, and for the $(Ti_{0,82}Zr_{0,18})N$ composition, the lattice period is 0.4311 nm. Thus, with an increase in the bias potential, there is a slight rise in the relative content of the heavier element, Zr.

As the base for the study the system of (TiZr)N/ZrN multiperiod nanocomrosites was taken. In this system, one of the layers was ZrN, and the other was (TiZr) solid solution nitride. Due to the large difference in the atomic radii of titanium (0.147 nm) and zirconium (0.160 nm), in this case, an increase in the relative content of Ti leads to an increase in the mismatch of the lattice periods in the contacting layers. The same effect of period mismatch was obtained in (TiZr)N/MoN nanocomposites.

Fig. 2 shows the diffraction spectra of nanocomposite (TiZr)N/ZrN coatings deposited at the smallest layer thickness (about 8 nm) and bias potentials (-70 V, -120 V and -220 V). Analysis of the obtained diffraction spectra showed that crystallites in the layers have a similar structural type (B1-NaCl, based on an fcc crystal lattice with the introduction of nitrogen atoms into octahedral interstices). The formation of this structural type is characteristic of the vacuum-arc method of nitride coatings formation [23-24], since such a lattice is highly resistant to nonstoichiometry.

The obtained diffraction spectra of (TiZr)N/ZrN nanocomposites with the smallest layer thickness showed two regularities: with an increase in the bias potential, the (TiZr)N diffraction peaks shift towards larger diffraction angles and the width of the diffraction peaks decreases. This is clearly seen from the spectra shown in Fig. 2, a. For comparison, a similar effect was obtained for ultrathin layers (about 8 nm) in the (TiZr)N/MoN composite (Fig. 2, b). In this case, a similar shift appears for γ-Mo$_2$N (PDF 25-1366) diffraction peaks. It should be noted that the ZrN component in the (TiZr)N/ZrN nanocomposite has stronger bonds between the metal and nitrogen (higher heat of formation) than in the (TiZr)N solid solution. In the (TiZr)N/MoN nanocomposite, on
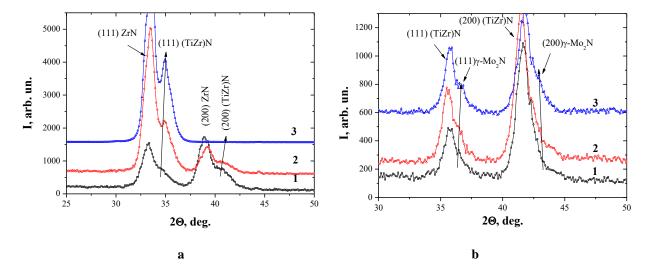

Fig. 2. Diffraction spectra of a multi-period (TiZr)N/ZrN (a) and (TiZr) (TiZr)N/MoN (b) nanocomposite with a layer thickness of about 8 nm (a) and about 80 nm (b): 1 – U_b = -70 V, 2 – U_b = -120 V, 3 – U_b = -220 V.

the contrary, the binding force (and, accordingly, the heat of formation) in the molybdenum nitride layer is lower (the formation of a γ-Mo$_2$N phase with a cubic lattice of the B1-NaCl structure type is characteristic of vacuum-arc coatings of molybdenum nitride [25]. This suggests that the observed effects of an increase in the diffraction angle (associated with a decrease in the lattice period) with an increase in U_b is determined by a change in the interaction conditions between nano-scale layers, predominantly passing in layers with a lower interatomic bond energy (and, accordingly, a lower elastic modulus).

With thicker layers (about 80 nm), as can be seen from Fig. 3 for the (TiZr)N/MoN nanocomposite, a similar effect of an increase in the displacement of the peaks of the (TiZr)N phase with increasing U_b is not observed.

Thus, for coatings deposited with the shortest layer formation time (continuous rotation) with a layer thickness of about 8 nm, with increasing U_b, the relative difference between the lattice constants of ZrN (layers) and (TiZr)N layers increases (spectra 1, 2, and 3 in Fig. 2, a). At $U_b = -70$ V and the smallest layer thickness, the difference in periods is $\delta = 0.4629 - 0.4431 = 0.0188$ nm. At $U_b = -120$ V, the difference increases to $\delta = 0.4625 - 0.4411 = 0.0214$ nm, and at $U_b = -220$ V, this difference is $\delta = 0.4614 - 0.4379 = 0.0235$ nm.

It is known that nanoperiodic composites are characterized by coherent conjugation of boundaries, when the periods are adjusted in the interlayer region and a superstructural state is obtained [26-28]. The appearance of δ indicates a transition to a partially coherent boundary (usually with a large mismatch of periods in the layers) [29–30]. In this regard, the observed increase in δ (with increasing U_b) indicates a decrease in the degree of such coherent conjugation of crystal lattices in adjacent ZrN/(TiZr)N layers with increasing U_b.

At the same time, in relatively thick layers (about 80 nm, Fig. 3), the δ value for all U_b has a large value $\delta \approx 0.026$ nm, which is close for this type of lattice without coherent conjugation. Thus, with a large layer thickness, the (TiZr)N crystal lattice has a period close to the calculated one (0.4231 nm) for this composition. This indicates a low level of coherent conjugation. An increase in U_b leads to the fact that the level of coherent conjugation also decreases between ultrathin layers.

This effect can be more clearly visualized when comparing the spectra after their decomposition into components. Fig. 4 shows the diffraction spectra of coatings obtained at $U_b = -70$ V (Fig. 4, a, b), -120 V (Fig. 4, c, d) and -220 V (Fig. 4, e, f) for coatings of two types with ultra-small thickness (about 8 nm) and relatively large thickness (about 80 nm).

The analysis of the substructural characteristics carried out on the basis of the separated spectra showed that, in composites with ultrathin layers (about 8 nm), with increasing U_b, the microstrain decreases. For the constituent ZrN layers, microstrain decreases from $\langle\varepsilon\rangle = 1.86$ % (at $U_b = -70$ V) to $\langle\varepsilon\rangle = 1.36$ % (at $U_b = -220$ V). In the (TiZr)N layer, microstrain decreases from $\langle\varepsilon\rangle = 1.46$ % (for $U_b = -70$ V) to $\langle\varepsilon\rangle = 1.33$ % (at $U_b = -220$ V). In composites with thicker layers (about 80 nm) ZrN layers with increasing U_b, the microstrain decreases from $\langle\varepsilon\rangle = 1.24$ % ($U_b = -70$ V) to $\langle\varepsilon\rangle = 0.52$ % ($U_b = -220$ V). In the (TiZr)N layers composing the composite, microstrain decreases from $\langle\varepsilon\rangle = 0.85$ % ($U_b = -70$ V) to $\langle\varepsilon\rangle = 0.41$ % ($U_b = -220$ V). The average crystallite size in the (TiZr)N layers is almost 2 times smaller than in the ZrN layers and is 25...29 nm.

With an increase in the constant potential, the crystallite size growth is observed, this is associated with an increase in the energy of incident particles, which leads to an increase in the mobility of atoms.

Thus, the use of ultrathin layers in nanocomposites makes it possible to design the interlayer structural state using bias potential of different magnitude.

With a relatively low value of such a potential -70...-220 V with increasing U_b, the difference in periods in adjacent layers increases. This can be explained by the loss of coherent conjugation between layers. The reason for this may be an increase in the mobility of deposited
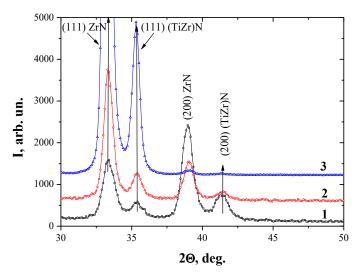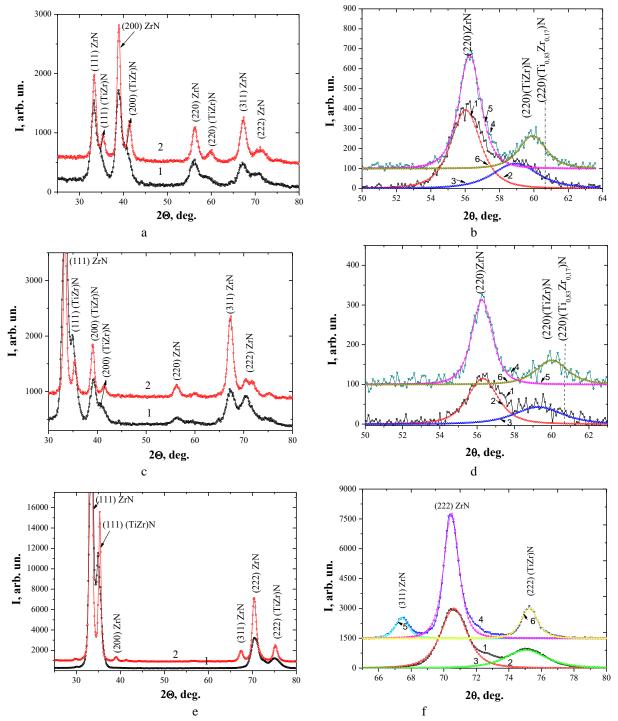

Fig. 3. Diffraction spectra of a multi-period (TiZr)N/MoN nanocomposite with a layer thickness of about 80 nm:
1 – $U_b = -70$ V, 2 – $U_b = -120$ V, 3 – $U_b = -220$ V.

O.V. Sobol', H.O. Postelnyk, N.V. Pinchuk, A.A. Meylekhov, M.A. Zhadko, A.A. Andreev, V.A. Stolbovoy

1 – initial profile (8 nm thick coating), 2 and 3 – profiles after decomposition,
4 – initial profile (80 nm thick coating), 5 and 6 – profiles after decomposition

Fig. 4. Diffraction spectra of nanocomposite (TiZr)N/ZrN coatings after decomposition into components at a thickness of about 8 nm (spectra 1) and about 80 nm (spectra 2): a, b – U_b = -70 V, c, d – U_b = -120 V, e, f – U_b = -220 V.

particles with increasing U_b, which contributes to the formation of a more equilibrium state of nitrides (solid solution with a lattice period characteristic of such a state).

Conclusions

1. The influence of the bias potential has a decisive effect on the structure and substructural characteristics of single-layer ZrN vacuum-arc coatings. With an increase in U_b in the range -70 ... -220 V, a texture with the [111] axis is formed, and the perfection of the substructure increases (an increase in the average crystallite size and a decrease in microstrain). The revealed effect is associated with an increase in the kinetic energy of the deposited particles, which contributes to an increase in their mobility with the formation of a preferred orientation of

crystallites from the most closely packed (111) plane and an increase in the perfection of the crystallite substructure.

2. During the formation of a ZrN/(TiZr)N nanocomposite, with an increase in U_b, the degree of texturing with the [111] axis in the layers also increases, and at the substructural level, the average crystallite size increases and microstrain decreases. In this case, in the layers of the ((TiZr)N) solid solution nitride, the values of microstrain and crystallite size are almost 1.5 times lower.

3. In ultrathin (about 8 nm thick) layers of nanocomposites, the effect of an increase in the interlayer mismatch δ with increasing U_b is revealed. This effect indicates that when U_b changes in the range -70 ... -220 V, the particles, increasing their energy during deposition, stimulate the relaxation of the interlayer deformation of the crystal lattices of the mating materials. This leads to their more equilibrium state with a lattice period close to the equilibrium one for a given composition (for a (TiZr)N solid solution nitride, the calculated period is 0.431 nm).

Sobol' O.V. - Ph.D., Professor of the Department of Materials Science;
Postelnyk H.O. - junior researcher of the Department of Materials Science;
Pinchuk N.V. - junior researcher of the Department of Materials Science;
Meylekhov A.A. - junior researcher of the Department of Materials Science;
Zhadko M.A. - Ph.D., junior researcher of the Department of Materials Science;
Andreev A.A. - Doctor of Technical Sciences, Senior Researcher;
Stolbovoy V.A. - Ph.D., head of the laboratory.

[1] B.D. Morton, H. Wang, R.A. Fleming, M. Zou, Tribology letters 42(1), 51 (2011) (https://doi.org/10.1007/s11249-011-9747-0).
[2] O.V. Sobol, A.A. Andreev, V.F. Gorban, A.A. Meylekhov, H.O. Postelnyk, V.A. Stolbovoy, Journal of Nano- and Electronic Physics 8(1), 1042 (2016) (https://doi.org/10.21272/jnep.8(1).01042).
[3] O.V. Sobol, A.A. Postelnyk, A.A. Meylekhov, A.A. Andreev, V.A. Stolbovoy, V.F. Gorban, Journal of nano- & electronic physics 9(3), 03003 (2017) (https://doi.org/10.21272/jnep.9(3).03003).
[4] P.H. Mayrhofer, C. Mitterer, L. Hultman, H. Clemens, Progress in Materials Science 51, 1032 (2006) (https://doi.org/10.1016/j.pmatsci.2006.02.002).
[5] P.H. Mayrhofer, D. Music, J.M. Schneider, Appl. Phys. Letter. 88, 071922 (2006) (https://doi.org/10.1063/1.2409364).
[6] O.V. Sobol', A.A. Andreev, V.F. Gorban', V.A. Stolbovoy, A.A. Melekhov, A.A. Postelnyk, Technical physics 61(7), 1060 (2016) (https://doi.org/10.1134/S1063784216070252).
[7] A.O. Eriksson, J.Q. Zhu, N. Ghafoor, J. Jensen, G. Greczynski, M.P. Johansson, J. Sjolen, M. Oden, L. Hultman, J. Rosen, Journal of Materials Research 26, 874 (2011) (https://doi.org/10.1557/jmr.2011.10).
[8] Q. Zhu, A.O. Eriksson, N. Ghafoor, M.P. Johansson, G. Greczynski, L. Hultman, J. Rosen, M. Oden, Journal of Vacuum Science and Technology A 29, 031601 (2011) (https://doi.org/10.1116/1.3569052).
[9] V. Braic, A. Vladescu, M.Balaceanu, C.R.Luculescu, M.Braic, Surface and Coatings Technology 211, 117 (2012) (https://doi.org/10.1016/j.surfcoat.2011.09.033).
[10] O.V. Sobol, A.A. Andreev, V.F. Gorban, Metal Science and Heat Treatment 58(1), 37 (2016) (https://doi.org/10.1007/s11041-016-9961-3).
[11] O.V. Sobol', A.A. Meilekhov, Technical Physics Letters 44(1), 63 (2018) (https://doi.org/10.1134/S1063785018010224).
[12] M.A. Al-Bukhaiti, K.A. Al-Hatab, W. Tillmann, F. Hoffmann, T. Sprute, Appl. Surf. Sci. 318, 180 (2014) (https://doi.org/10.1016/j.apsusc.2014.03.026).
[13] X. Chu, S.A. Barnett, J. Appl. Phys. 77, 4403 (1995) (https://doi.org/10.1063/1.359467).
[14] Y.Z. Tsai, J.G. Duh, Thin Solid Films 518, 7523 (2010) (https://doi.org/10.1016/j.tsf.2010.05.038).
[15] Q. Luo, Wear 271, 2058 (2011) (https://doi.org/10.1016/j.wear.2011.01.054).
[16] Y. Qiu, S. Zhang, J.W. Lee, B. Li, Y. Wang, D. Zhao, Appl. Surf. Sci. 279, 189 (2013) (https://doi.org/10.1016/j.apsusc.2013.04.068).
[17] S. Zhang, D. Sun, Y. Fu, H. Du, Surf. Coatings Technol. 167, 113 (2003) (https://doi.org/10.1016/S0257-8972(02)00903-9).
[18] J. Patscheider, MRS Bull. 2, 180 (2003) (https://doi.org/10.1557/mrs2003.59).
[19] E. Liu, J. Pu, Z. Zeng, Y. Wang, W. Zhao, Surf. Eng. 33, 633 (2017) (https://doi.org/10.1080/02670844.2017.1292704).
[20] O.V. Sobol', O.A. Shovkoplyas, Technical Physics Letters 39(6), 536 (2013) (https://doi.org/10.1134/S1063785013060126).
[21] http://www.icdd.com.
[22] L.S. Palatnik, M.Ya. Fuks, V.M. Kosevich, Mekhanizm obrazovaniya i substruktura kondensirovannykh plenok (Nauka, Moscow, 1972).

O.V. Sobol', H.O. Postelnyk, N.V. Pinchuk, A.A. Meylekhov, M.A. Zhadko, A.A. Andreev, V.A. Stolbovoy

[23] O.V. Sobol, A.A. Andreev, V.F. Gorban, A.A. Meylekhov, H.O. Postelnyk, V.A. Stolbovoy, Nano- and Electronic Physics 8(1), 01042 (2016) (https://doi.org/10.21272/jnep.8(1).01042).
[24] O.V. Sobol, A.A. Postelnyk, A.A. Meylekhov, A.A. Andreev, V.A. Stolbovoy, V.F. Gorban, Journal of nano- & electronic physics 9(3), 03003 (2017) (https://doi.org/10.21272/jnep.9(3).03003).
[25] O.V. Sobol, A.A. Andreev, V.A. Stolbovoi, V.E. Fil`chikov, Technical physics letters 38(2), 168 (2012). (https://doi.org/10.1134/S1063785012020307).
[26] R. Hahn, M. Bartosik, R. Soler, Scripta Materialia 124, 67 (2016) (https://doi.org/10.1016/j.scriptamat.2016.06.030).
[27] P. Eh. Hovsepian, D.B. Lewis, Q. Luo, A. Farinotti, Thin Solid Films 488(1-2), 1 (2005) (https://doi.org/10.1016/j.tsf.2005.03.016).
[28] Chang-Lin Liang, Guo-An Cheng, Rui-Ting Zheng, Hua-Ping Liu, Thin Solid Films 520, 813 (2011) (https://doi.org/10.1016/j.tsf.2011.04.159).
[29] Yu X. Xu, Li Chen, Zi Q. Liu, Fei Pei, Yong Du, Surface and Coatings Technology 321, 180 (2017) (https://doi.org/10.1016/j.surfcoat.2017.04.057).
[30] M. Stueber, H. Holleck, H. Leiste, K. Seemann, S. Ulrich, C. Ziebert, Journal of Alloys and Compounds 483(1-2), 321 (2009) (https://doi.org/10.1016/j.jallcom.2008.08.133).

О.В. Соболь[1], Г.О. Постельник[1], Н.В. Пінчук[1], А.О. Мейлехов[1],
М.О. Жадко[1], А.О. Андреєв[2], В.О. Столбовий[2]

Вплив величини потенціалу зсуву на структурну інженерію вакуумно-дугових покриттів на основі ZrN

[1]Національний технічний університет "Харківський політехнічний інститут", Харків, Україна, sool@kpi.kharkov.ua
[2]Національний науковий центр "Харківський фізико-технічний інститут", Харків, Україна, stolbovoy@kipt.kharkov.ua

Створення наукових основ структурної інженерії надтонких наношарів в багатошарових нанокомпозитах є основою сучасних технологій формування матеріалів з унікальними функціональними властивостями. Показано, що збільшення від'ємного потенціалу зсуву (від -70 до -220 В), при формуванні вакуумно-дугових нанокомпозитів на основі ZrN, дозволяє не тільки управляти переважною орієнтацією кристалітів і субструктурними характеристиками, але і змінює умови сполучення кристалічних решіток в надтонких (близько 8 нм) наношарах.

Ключові слова: вакуумна дуга, нітрид цирконію, багатошарові нанокомпозити, рентгеноструктурний аналіз, наноструктура, міжшарове сполучення, текстура, субструктура.